Characteristic molecular weights in the dynamics of polymer melts: n.m.r. and zero-shear viscosity

R. Kimmich
Universität Ulm, Sektion Kernresonanzspektroskopie, Postfach 4 066, D-7900 Ulm West Germany
(Received 30 March 1983)

As shown in previous papers, chain fluctuations in polymer melts can be analysed into three consecutive components (local segment re-orientation, reptation within the tight tube and tube renewal). The intensity function derived on this basis leads to a series of limiting cases, which can be realized by frequency and/or molecular weight variation. The occurrence of the characteristic molecular weights M_{AB}, M_{BC} and M_c separating these limits have been verified by the aid of nuclear magnetic relaxation of linear polyethylene and atactic polystyrene melts. The M_c-values are equivalent to the critical molecular weights as known from rheology. An expression for the zero-shear viscosity in the whole range of molecular weights has been derived.

Keywords Nuclear magnetic relaxation spectroscopy; zero-shear viscosity; molecular weight dependence; polymer melts; reptation; contour length fluctuation

INTRODUCTION

The classical critical molecular weight, M_c, is shown, for example, by a break in the molecular weight dependence of the zero-shear viscosity[1,2]. However, M_c is not the only molecular weight indicating a transition between different molecular weight dependences of dynamic quantities. In previous papers[3,4] it has been shown that the nuclear magnetic relaxation times T_1 and T_2 are influenced by additional characteristic molecular weights, which are designated M_{AB} and M_{BC}. All three characteristic molecular weights can be understood as transitions between dynamic limits based on three motional components, which will be described in the following.

A tight tube[4] surrounding a reference chain is defined by the space occupied, on average, by this chain in the time scale of the local and, therefore, molecular weight independent processes. Apart from sidegroup motions, local processes are considered to be mainly due to local defect diffusion[4,5]. Fluctuations of this type are called 'component A' (*Figure 1*). Component A is anisotropic and, hence, causes a decay of the segment orientation correlation function only down to a certain residual correlation. The essence of a tube model of this type is that the residual correlation can be maintained over times many orders of magnitude longer than the time scale of component A. In the following the term 'tight tube' is used to avoid any confusion with definitions of more extensive tubes introduced elsewhere[6].

Defect diffusion is the elementary process which finally causes the reptation phenomenon[7-9]. Segment displacements on this basis occur along the axis of the tight tube. If they exceed the correlation length of the tight tube orientation, the residual correlation of the segment orientation left over by component A will decay further towards zero[10]. This process is called 'component B' (*Figure 1*). Thus, in contrast to component A, which is based more directly on thermal activation, component B is considered as a secondary process.

Reptation finally leads to tertiary processes which are competitive to component B. First, reptation can represent material transport to or from chain ends, so that it causes tube renewal[7] and, hence, the definitive loss of correlation to the initial segment orientation. The

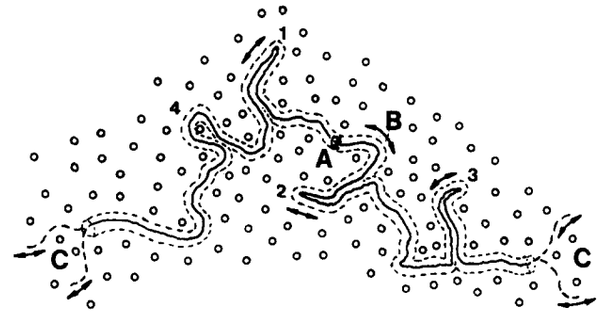

Figure 1 Schematic illustration of a chain in polymer melts. The chain is confined into a tight tube formed by the matrix of neighbouring chains (circles). The diameter of the tight tube is given by the mean fluctuation amplitude of the local (molecular weight independent) processes. These are designated as *component A*. It mainly represents anisotropic re-orientations by local defect diffusion. *Component B* is due to further re-orientation by reptative displacements around bends of the tight tube. *Component C* finally causes the definitive correlation loss by tube renewal. The chain threads into a new conformation by whole-chain reptation (relevant mainly in the inner section of the chain) or by contour-length fluctuation (relevant near chain ends). The contour length is the tube length minus the length stored in folds. A fold is a lateral extension not entangled by a neighbouring chain. Thus, the numbers 1 to 3 indicate folds (growth and shrinkage fluctuation possible), while 4 is no fold (no fluctuation degree of freedom). The arrows indicate the displacements connected with the diverse chain fluctuations.

0032-3861/84/020187-08$03.00

displacement of the whole chain by material transport via defect diffusion from chain end to chain end will be called 'whole-chain reptation'.

However, material transport can also occur between chain ends and 'folds' (*Figure 1*)[4]. A fold is any lateral extension of a chain which does not entangle neighbouring chains. Folds, therefore, can grow or shrink at any position along the tight tube and without strong distortion of the matrix. The fluctuation of the chain ends back and forth as a consequence of fold fluctuation again means that the chain ends thread into a new tube[11]. This type of 'internal' reptation will be called 'contour length fluctuation' where contour length means the tight-tube length minus the lengths stored in folds (*Figure 1*).

Both types of tube renewal are comprised within the term 'component C'. Note that component C refers to the definitive tube renewal process, while the tube renewal experienced by the segments situated in a growing or shrinking fold is only temporary and can completely be reversed within the same entanglement network (*Figure 1*). Thus, growth or shrinkage of folds directly contribute to component B, but only indirectly to component C as an effect of the whole fold ensemble of a chain.

The three components generally allow the nuclear magnetic relaxation behaviour of polymer melts to be described[4,12]. For this purpose the correlation function of the segment orientation is given by:

$$G(t)=G_A(t)G_B(t)G_c(t) \tag{1}$$

and the intensity function:

$$I(\omega)=\int_{-\infty}^{\infty} G(t)\exp^{-i\omega t}\,dt \tag{2}$$

G_A, G_B and G_c are the partial correlation functions of the three components, which will be specified later. Here, it is assumed that the three components are stochastically independent in spite of the hierarchy of elementary, secondary and tertiary processes. However, the hierarchic sequence of the components means that the components are connected with completely different time scales. Any correlation between them, therefore, can be neglected.

The correlation function approach, equation (1), to chain fluctuations in polymer melts is opposed by the classic relaxation mode concept[13-15]. The advantage of this approach is that infinite series of discrete mode expressions are avoided, though the argument occasionally implies simplifications.

CORRELATION FUNCTIONS

Component A refers to local motions such as the diffusion of defects over short distances and, if relevant, sidegroup motions. By a computer simulation[4,9] it may be shown that in the short-time limit, defect diffusion approximately corresponds to the diffusion of a particle between two reflecting barriers[16]. The reflecting barriers here represent the quasi-static ensemble of neighbouring defects. The result is a relaxation process, the width of which is determined by the mean diffusion time over the distance of the reflecting barriers. As the time constants of the other components must be longer than this diffusion time, the long-time behaviour of component A can be described by a simple exponential function with an anisotropy constant:

$$G_A(t)=a_1\exp(-t/\tau_s)+a_2 \tag{3}$$

where $a_1+a_2=1$. τ_s is an effective time constant characterizing the long-time behaviour and the constants a_1 and a_2 are determined by the degree of anisotropy of component A. Note that only a non-zero value of a_2 permits the detection of further fluctuation components.

Component B or reptation around tube bends is described by[8,10]:

$$G_B(t)=\exp(t/2\tau_l)\,\mathrm{erfc}\,(t/2\tau_l)^{1/2} \tag{4}$$

with $\tau_l=l^2/2D_1^{(l)}$. τ_l is the mean diffusion time over the correlation length l of the tight-tube orientation. Here, it is assumed that the chain diffuses with a constant diffusion coefficient $D_1^{(l)}$ within a stationary tube of infinite length. The assumption of an infinite tube is justified because any tube renewal process is attributed to component C which is of a competitive nature to component B. The stationarity of the tight-tube conformation is more problematic as it contradicts the growth or shrinkage of folds as discussed previously. Rather the fluctuation of a fold in principle can contribute to component B. However, the correlation length of the tight-tube orientation is expected to be so short, that reptative displacements around tight-tube bends will be fast compared with fold fluctuation (also, it is unlikely that the reference segment is situated in a fold at all). Note that equation (4) implies the possibility that the segment has *returned* to its initial tight tube orientation after time t. Thus, G_B decays extremely slowly allowing even tube renewal processes to be observed in spite of the absence of any additional anisotropy term.

Tube renewal (*component C*) leads to the definitive loss of correlation to the initial segment orientation. As shown in ref. 4 the two mechanisms contributing to component C dominate in different sections of the chain (*Figure 2*). A fraction p_r of the segments is situated in the range $x_r<x<L_0-x_r$ of the curvilinear tight-tube co-ordinate, where whole-chain reptation is the dominating tube renewal mechanism. L_0 is the tight-tube length, x_r is half the mean contour length fluctuation, which provides the dominating tube renewal process outside of that range.

The partial correlation functions of the whole-chain reptation mechanism and that due to contour length fluctuation are designated by C_r and C_c, respectively. These functions represent averages over their regions of dominance as shown in *Figure 2*. Thus, the average correlation function characterizing the total component C is given by:

$$G_c(t)=p_cC_c(t)+p_rC_r(t) \tag{5}$$

with $p_c=2x_r/L_0$ and $p_r=1-p_c$.

The formation of the averages implied in equation (5) is justified for considerations of the proton spin–lattice relaxation time T_1. Here, spin diffusion[17] guarantees that

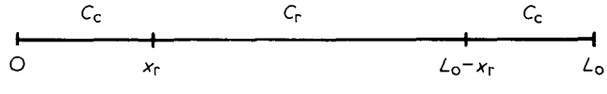

Figure 2 Distinction of three chain sections concerning the tube renewal mechanisms

the average is observed over all relaxation heterogeneities along a chain, so that the average formally can already be carried out on the level of the correlation functions. With dilute nuclei and with the transverse relaxation time this argument no longer holds. Rather, a distribution of correlation functions should be used leading to a distribution of relaxation times.

As shown later, either the first or the second term of equation (5) can be neglected for $M \gg M_c$ and $M \ll M_c$, respectively, where M_c is the classical critical molecular weight[1,2]. Thus, this objection is irrelevant in these limiting cases. If $M \approx M_c$, however, both terms will be of equal importance and strongly non-exponential T_2-relaxation curves are expected. Later, there is a brief discussion of an experimental result fitting this prediction.

For tube renewal by the whole-chain reptation mechanism the correlation function is given by:

$$C_r(t) = \langle 1 - \{P(x,t) + P(L_0 - x, t) - P(x, L_0 - x, t)\} \rangle_x \quad (6)$$

The average concerns the curvilinear tight-tube coordinate x in the range $x_r < x < L_0 - x_r$ (*Figure 2*). The part of the equation within the braces represents the probability that either one of the two chain-ends or both have reached the initial position of the reference segment during the interval t. The complementary probability averaged over all reference segments thus represents the correlation function $C_r(t)$. $P(x,t)$ and $P(L_0-x,t)$ consequently are the probabilities that *one* chain end attains a distance of at least x or (L_0-x), respectively, at least once during t. $P(x, L_0-x, t)$ is the probability that *both* chain ends do so.

Thus, the part of the equation within the braces in equation (6) represents the equivalent of a one-dimensional particle diffusion problem with a *two-sided* absorbing wall. Here, the displacements of the chain ends are considered. Alternatively, it is possible to treat the diffusion of the reference segment which then has to be considered to migrate between *two* absorbing walls. This assumption has been used in ref. 18. However, this type of treatment results in an infinite series of diffusion modes which is undesirable here.

Equation (6) can be simplified by realizing that $P(x, L_0-x, t) \ll 1$ for $t < \tau_L$ and $P(x, L_0-x, t) \approx P(x,t)P(L_0-x,t)$ for $t > \tau_L$, where τ_L is the mean diffusion time over a curvilinear displacement in the order of L_0. Replacing, furthermore, the average by the expression for the central chain segment, which is justified in view of the relatively weak x-dependence in the section $x_r < x < L_0 - x_r$, thus[4,19]:

$$C_r(t) \approx \langle [1 - P(x,t)][1 - P(L_0 - x, t)] \rangle_x \approx \left\{ \mathrm{erf} \sqrt{\frac{\tau_r^r}{t}} \right\}^2 \quad (7)$$

with $\tau_r^r = (L_0 - 2x_r)^2 / \gamma_r D_1$ (D_1 curvilinear whole-chain diffusion coefficient, γ_r numerical factor of the order of 10).

To obtain the intensity function, the total correlation function, equation (1), has to be Fourier transformed (equation (2)). For this purpose the partial correlation function, equation (7) was unsuitable. Therefore, it was replaced by an exponential term:

$$C_r(t) \approx \exp(-t/\tau_r^r) \quad (8)$$

where τ_r^r now implies a slightly modified numerical factor γ_r which is irrelevant for scaling-law considerations. Initially, the simplification step from equation (7) to equation (8) appears to be severe. However, a numerical comparison of the total three-component intensity function based on equations (7) and (8), respectively, showed that perfect coincidence can be attained simply by appropriately choosing the numerical factor γ_r[19].

The correlation function for tube renewal by contour length fluctuation, i.e. for segments virtually situated in the outer chain segments, the assumption[4] is made that:

$$C_c(t) = \exp(-t/\tau_r^c) \quad (9)$$

with $\tau_r^c = 4x_r^2/\gamma_c D_1^{(0)}$. $D_1^{(0)}$ is the curvilinear diffusion coefficient of the outer chain sections which is *effective in the time scale of contour length fluctuation.* Note the difference to D_1 which concerns displacements of the whole chain. γ_c is again a numerical factor of the order of 10. Exponential correlation functions of this type are also used in connection with density fluctuations[20,21], which are equivalent to contour length fluctuation.

The mean contour length fluctuation is[4]:

$$2x_r = (L_0 \Delta_0)^{1/2} \quad (10)$$

where Δ_0 is the mean tube length per fold. Thus, by combining equations (1), (3)–(5), (8) and (9), the total three-component correlation function is obtained in a version which is suitable for Fourier transformation:

$$G(t) = [a_1 \exp(-t/\tau_s) + a_2] \times \exp(t/2\tau_l)\,\mathrm{erfc}\,(t/2\tau_l)^{0.5} \times [(\Delta_0/L_0)^{1/2} \exp(-t/\tau_r^c) + (1 - \sqrt{\Delta_0/L_0}) \times \exp(-t/\tau_r^r)] \quad (11)$$

The time constants are of different orders of magnitude as a consequence of the hierarchic sequence of the components. Especially it holds for $\tau_s \ll \tau_r^c, \tau_r^r$. Then, the intensity function is[4,12]:

$$I(\omega) = \sum_{j=1}^{4} \gamma_j [2\tau_c^{(j)} + \tau_c^{(j)3/2} \tau_l^{-1/2} (1 + K^{(j)})^{1/2}] \div \{K^{(j)^2} + \tfrac{1}{2}\tau_c^{(j)} \tau_l^{-1} K^{(j)} + \tau_c^{(j)1/2} \tau_l^{-1/2} \times [(1 + K^{(j)})^{1/2} + \omega \tau_c^{(j)} (K^{(j)} - 1)^{1/2}]\} \quad (12)$$

where $K^{(j)} = (1 + (\omega \tau_c^{(j)})^2)^{1/2}$

$\tau_c^{(1)} \approx \tau_c^{(2)} \approx \tau_s$

$\tau_c^{(3)} = \tau_r^c$

$\tau_c^{(4)} = \tau_r^r$

$\gamma_1 = a_1 (\Delta_0/L_0)^{1/2}$

$\gamma_2 = a_1 (1 - (\Delta_0/L_0)^{1/2})$

$\gamma_3 = a_2 (\Delta_0/L_0)^{1/2}$

$\gamma_4 = a_2 (1 - (\Delta_0/L_0)^{1/2})$

Depending on ω and the time constants in equation (12), different limiting cases can be derived. As the diverse time constants have different molecular weight dependences, it is possible to realize the limiting cases by the appropriate choice of the chain length. Then, it is possible to attribute characteristic molecular weights to the case transitions as shown later.

LIMITING CASES AND CHARACTERISTIC MOLECULAR WEIGHTS

From equation (12) a series of limiting cases can be derived. The general condition representing the hierarchy of the three-component model is $\tau_r^c, \tau_r^r \gg \tau_l \gg \tau_s$. Additional conditions are given for the following limits:

Case 1: $\omega\tau_r^c \ll 1$ and $\gamma_3\tau_r^{c1/2} \gg \gamma_4\tau_r^{r1/2}$

$$I(\omega) \approx 2a_2\left(\frac{2\Delta_0\tau_l\tau_r^c}{L_0}\right)^{1/2} \tag{13a}$$

This case is valid for small frequencies and short chain-lengths. It is then component B and C (tube renewal mainly by contour length fluctuation) which determine the intensity function. If tube renewal is governed by the competitive mechanism, i.e. whole-chain reptation, then:

Case 2: $\omega\tau_r^r \ll 1$ and $\gamma_3\tau_r^{c1/2} \ll \gamma_4\tau_r^{r1/2}$

$$I(\omega) \approx 2a_2\left(1-\left(\frac{\Delta_0}{L_0}\right)^{1/2}\right)(2\tau_l\tau_r^r)^{1/2} \tag{13b}$$

This is still valid at small frequencies, but longer chains are required to realize this situation. Note that in both cases the effective time constant appears as the geometric average of the time constants of components B and C.

Higher molecular weights and/or greater frequencies lead to:

Case 3: $\omega\tau_r^c \gg 1$, $\omega\tau_r^r \gg 1$, $\omega\tau_s \ll 1$, $\omega\tau_l \ll 1$

$$I(\omega) \approx (2a_1\tau_s) + 2a_2\omega^{-1/2}\tau_l^{1/2} \tag{13c}$$

The first term is minor provided the frequency is sufficiently low. Then it is component B alone which dominates in the intensity function.

The following cases refer to essentially higher frequencies allowing consideration of the condition $\omega\tau_l \gg 1$:

Case 4: $\omega\tau_r^c \gg 1$, $\omega\tau_r^r \gg 1$, $\omega\tau_s \ll 1$, $\omega\tau_l \gg 1$

$$I(\omega) \approx 2a_1\tau_s + a_2\omega^{-3/2}\tau_l^{-1/2} \tag{13d}$$

It is now components A and B which determine the intensity function. Depending on the numerical values of a_1 and a_2, the frequency and the chain length, situations might arise where either the first or the second term dominates. Thus:

Case 4a: $$I(\omega) \approx a_2\omega^{-3/2}\tau_l^{-1/2} \tag{13e}$$

and

Case 4b: $$I(\omega) \approx 2a_1\tau_s \tag{13f}$$

Increasing the frequency and/or the molecular weight, in principle provides the possibility to attain all cases subsequently. The respective characteristic molecular weights are designated as follows:

Case 1–2: M_c

Case 2–3: M_{BC}

Case 4a–4b: M_{AB}

The subscripts indicate the components involved with the transitions. Clearly, the case transitions indicated by the characteristic molecular weights will partially depend on frequency and temperature. M_{BC} and M_{AB} (but not M_c) consequently will be functions of these experimental parameters. As the components and the mechanisms are characterized by different dependences on the chain length, it is expected that the characteristic molecular weights are shown by clear breaks in the molecular weight dependence of quantities based on the intensity function.

EXPERIMENTAL

The n.m.r. spectrometers and the methods used for this study have been described elsewhere[5]. The (linear) polyethylene fractions (PE) in part were given by Dr Goldbach, Hüls AG, Marl, FRG and Dr Asbach, Experimentelle Physik, Universität Ulm. The rest was purchased from Knauer, West Berlin, Polymer Laboratories, Shawbury, UK and Humphrey, North Haven, Conn., USA. The ratios of the weight and number averages of the molecular weights, M_w/M_n, ranged from 1.1 to 1.5. Results from gel permeation chromatography of some of the samples have been published previously[22]. The (atactic) polystyrene samples (PS) were either given by Dr Münstedt, BASF, Ludwigshafen or purchased from Knauer, West-Berlin and Pfannenschmidt, Hamburg. The ratio M_w/M_n was always $\lesssim 1.1$. Samples of 1 cm^3 were pressed in a cylindric form and evacuated at least overnight, typically 2 or 3 days.

NUCLEAR MAGNETIC RELAXATION TIMES

The existence of the predicted characteristic molecular weights M_c, M_{BC} and M_{AB} can be verified by the nuclear magnetic relaxation times T_1 and T_2 which are direct functions of the spectral density[4,17]. *Figure 3* shows the low-frequency data for polyethylene melts. Two breaks corresponding to M_c and M_{BC} are evident, where the M_c-

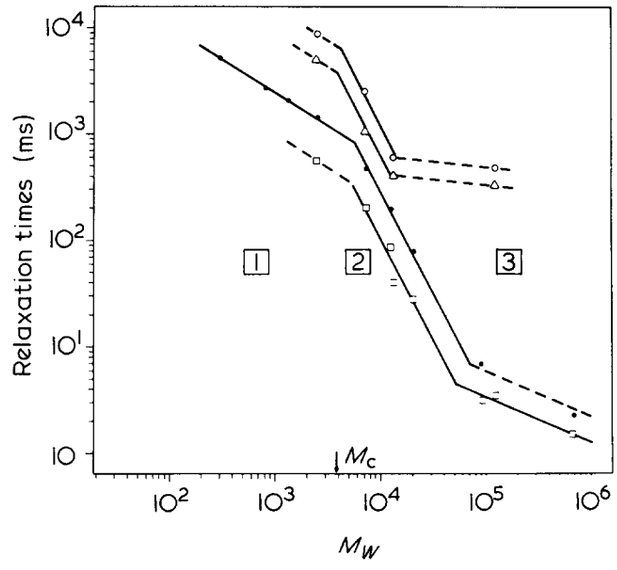

Figure 3 Molecular weight dependences of proton relaxation times T_1 (30 kHz) and T_2^* in polyethylene (T_2^* is the decay time to $1/e$ of the transverse magnetization measured by spin–echo techniques). The different slopes are interpreted by cases 1, 2 and 3 (see text). ○, $10\times T_1$, 200°C, 30 kHz; △, $10\times T_1$, 150°C, 30 kHz; ●, T_2^*, 200°C, 90 MHz; □, T_2^*, 150°C, 90 MHz

values are close to those reported in rheological studies[1,2].

Note that the frequencies relevant for the T_1-data are considerably higher than those relevant for T_2; in consequence the M_{BC}-values of the T_1-data are less than those of T_2 as predicted by equation (13c).

The slopes correspond to molecular weight dependences of the relevant parameters[4]:

$$\begin{aligned}\tau_s &= \kappa_s M_w^{0.0}\\ \tau_l &= \kappa_l M_w^{0.5\pm0.3}\\ \tau_r^c &= \kappa_r^c M_w^{1.7\pm0.3}\\ \tau_r^r &= \kappa_r^r M_w^{3.0\pm0.3}\end{aligned} \qquad (14)$$

The frequency dependence[4,12,22] of T_1 allows estimation of the order of magnitude of the constants κ_s, κ_l, κ_r^c and κ_r^r, so that a numerical computer fit is unnecessary. In the temperature range of the data of *Figure 3*, $\kappa_s \approx 10^{-10}$ s, $\kappa_l \approx 10^{-10}$ s, $\kappa_r^c \approx 10^{-13}$ s, $\kappa_r^r \approx 10^{-18}$ s. The residual correlation of component A is approximately $a_2 = 0.06$.

Below M_c, the molecular weight dependence of free volume[23] is also significant so that the power law given for τ_r^c should be considered to be unspecific. The molecular weight dependences of the curvilinear diffusion coefficients D_1 (equation (7)) and $D_1^{(0)}$ (equation (9)) for mean square displacements of the segments of the order of L_0^2 and x_r^2, respectively, can be derived from equation (14). In view of the additional free-volume M-dependence affecting $D_1^{(0)}$, it is evident that these results are completely compatible with the intrinsic power laws derived from model considerations[4,9]:

$$\begin{aligned}D_1 &\sim M_w^{-1}\\ D_1^{(0)} &\sim M_w^{-0.5}\end{aligned} \qquad (15)$$

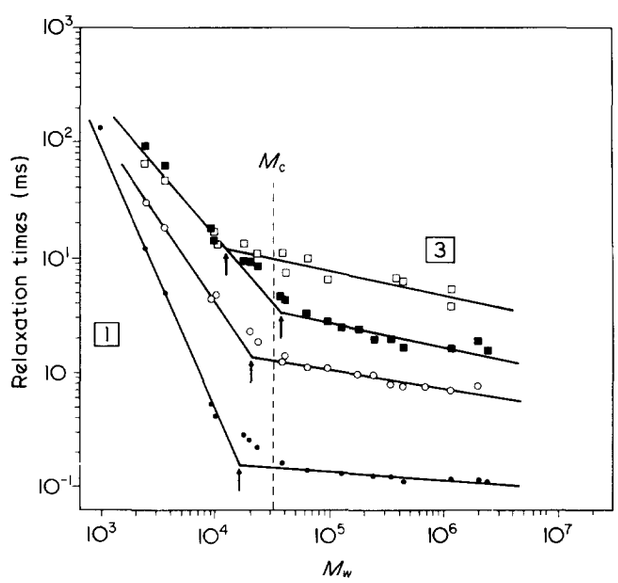

Figure 4 Molecular weight dependences of proton relaxation times T_1 (20 kHz) and T_2^* in polystyrene. The different slopes are interpreted by cases 1 and 3 (see text). As M_c is close to the values of M_{BC}, case 2 could not be resolved. A comparison with curves calculated on the basis of a somewhat simpler version of the complete three-component intensity function can be found in ref. 3. □, T_1, 200°C, 20 kHz; ■, T_2^*, 200°C, 40 MHz; ○, T_2^*, 174°C, 90 MHz; ●, T_2^*, 150°C, 40 MHz

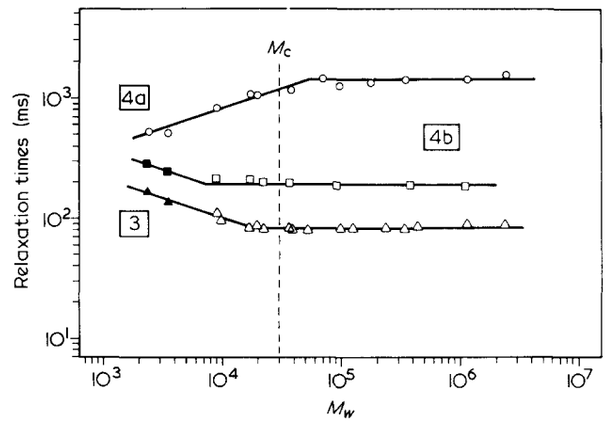

Figure 5 Molecular weight dependence of T_1 at 40 and 90 MHz in polystyrene. The different slopes are interpreted by cases 3, 4a and 4b (see text). At 200°C, case 4a obviously is not resolved. The filled symbols indicate slightly non-exponential relaxation curves, which have been approximately evaluated by a single (average) exponential function. M_c obviously has no influence because component C is ineffective in this frequency/temperature/molecular weight range. ○, $5\times T_1$, 150°C, 40 MHz; □, T_1, 200°C, 90 MHz; △, T_1, 200°C, 40 MHz

Figure 4 shows low-frequency relaxation data measured with polystyrene fractions. Only one break in each of the M-dependences is evident. Clearly, case 2 is not resolved. Rather, a direct transition is observed from case 1 (tube renewal by contour length fluctuation combined with component B) to case 3 (component B alone). The explanation for this finding is that the frequencies relevant for the relaxation times are so high that in this case $M_{BC} \lesssim M_c$. The prediction is that case 2 would be resolved if the experiment could be carried out for $\nu < 10^3$ Hz.

The M-dependences of τ_r^c, derived from the case 1 formula, leads to very high exponents[4] due to the strong influence of free volume in this polymer example[24]. The behaviour of τ_l corresponds to the power law found for polyethylene.

Figure 5 finally shows the high-frequency data for polystyrene. Here, case 3 is again evident, but now shifted to the lower end of the M_w-scale. Reduced frequencies and temperatures lead to the inverse power-law predicted by case 4a. (This transition is an equivalent to the symmetric V-type curve of the well-known T_1-minimum[17].) At high molecular weights case 4b is attained, which is governed by the molecular weight insensitive component A. The characteristic molecular weight, M_{AB}, is attributed to this transition. Note that case 4a is not resolved at 200°C. Rather, there is a direct transition from case 3 to case 4b at this temperature.

For 200°C:

$$\begin{aligned}\tau_s &= \kappa_s M_w^{0.0}\\ \tau_l &= \kappa_l M_w^{0.5\pm0.15}\\ \tau_r^c &= \kappa_r^c M_w^{2.8\pm0.2}\end{aligned} \qquad (16)$$

The order of magnitude of the constants are $\kappa_s \approx 10^{-9}$ s, $\kappa_l \approx 10^{-11}$ s, $\kappa_r^c \approx 10^{-16}$ s. Note that τ_s is an effective quantity which also refers to phenyl group motions. The residual correlation of component A is approximately $a_2 = 0.05$.

ZERO-SHEAR VISCOSITY

Zero-shear viscosity is determined by tube renewal (component C) alone[25]. Inserting equation (5) with the expressions for $C_c(t)$ and $C_r(t)$ into Doi's correlation function formula for the zero-shear viscosity η leads to:

$$\eta = K_1 L_0^2 \left(1 - \left(\frac{\Delta_0}{L_0}\right)^{0.5}\right)^3 \Big/ D_1 + K_2 \Delta_0^{1.5} L_0^{0.5} / D_1^{(0)} \quad (17a)$$

where K_1 and K_2 are constants with respect to chain length. The characteristic tube length L_0^c (corresponding to M_c) is then defined as the transition from a region where the second term dominates to that where the first term governs the viscous behaviour.

With the proportionalities in equation (15), therefore:

$$\eta = K_r L_0^3 (1 - (\Delta_0/L_0)^{0.5})^3 + K_c \Delta_0^{1.5} L_0$$

or

$$\eta \approx L_0 \quad (\Delta_0 < L_0 < L_0^c) \quad (17b)$$

$$\eta \approx L_0^{3.4} \quad (L_0^c < L_0 < 10^2 L_0^c)$$

i.e. the well known power laws are obtained for the zero-shear viscosity observed after eliminating the additional chain length dependence arising from free volume[1,2,24]. K_r and K_c are constants. The second proportionality implies an approximation[11] of the first term in equation (17a) by a power law effective in the range indicated. The quality of this approach is demonstrated in *Figure 6*. At even higher tube lengths a limiting power law[18] is expected:

$$\eta \sim L_0^3 \quad (L_0 \gg 10^2 L_0^c) \quad (18)$$

which, however, appears to be beyond the experimental accessibility.

With equations (17) and (13) there is a common basis for a discussion of nuclear magnetic relaxation times and zero-shear viscosity. A critical test of the fluctuation scheme is, therefore, to derive the molecular weight dependence of component C from n.m.r. relaxation times, to calculate the viscous behaviour on this basis and to compare it with rheological data, as shown in *Table 1*. The comparison shows that the model expressions are able to explain simultaneously the results of both methods, though they are influenced by the three components in a different way. Note that the molecular weight dependences in *Table 1* partially imply the additional M-dependence of free volume. The quantity mainly sensitive to free volume is $D_1^{(0)}$[4]. Note also that as a consequence of free volume, below M_c no pure power laws are valid. Rather, the proportionalities given in *Table 1* represent *average* dependences in the relevant M-ranges.

DISCUSSION AND CONCLUSIONS

The fluctuations relevant for chain dynamics in polymer melts are more complicated than hitherto assumed. Especially there is a variety of motional components and limiting cases which have to be considered in this context. The observation of the characteristic molecular weight M_{BC} as predicted by the three-component model and the successful 'translation' of the $T_1(M_w)$ and $T_2(M_w)$ relations to $\eta(M_w)$ strongly supports the scheme developed in a series of recent papers[4,8,10,12,19].

The explanation of the characteristic molecular weight M_c as a transition between two limits of tube renewal

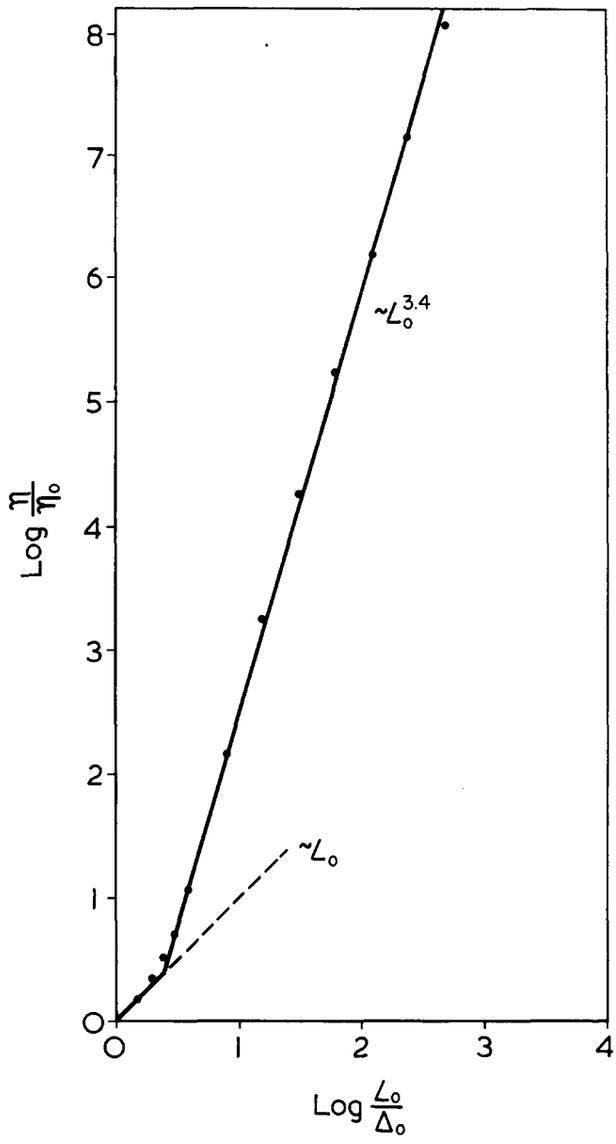

Figure 6 Chain-length dependence of the zero-shear viscosity. The points have been calculated with equation (17b) assuming $K_r = K_c = \Delta_0 = 1$. η_0 refers to $L_0 = \Delta_0$

Table 1 Comparison of the molecular weight dependences of the zero-shear viscosity derived from n.m.r. relaxation data and rheologically measured. The power laws below M_c must be considered to represent average molecular weight dependences including free-volume effects

	θ (°C)	η calc. from n.m.r. data (this work)	η directly measured (PS[26], PE[27–30])
PS ($M < M_c$)	140	–	$\sim M^{4.4 \pm 0.3}$
PS ($M < M_c$)	150	$\sim M_w^{4.5 \pm 0.3}$	–
PS ($M < M_c$)	155	–	$\sim M^{4.0}$
PS ($M < M_c$)	174	$\sim M_w^{2.9}$	–
PS ($M < M_c$)	190	–	$\sim M^{2.9}$
PS ($M < M_c$)	200	$\sim M_w^{2.3}$	–
PS ($M < M_c$)	217	–	$\sim M^{2.4}$
PS ($M > M_c$)	θ	–	$\sim M^{3.4}$
PE ($M < M_c$)	200	$\sim M_w^{1.24}$	$\sim M^{1.67}$
PE ($M > M_c$)	θ	$\sim M_w^{3.1}$	$\sim M^{3.4}$

without any structural change makes it plausible that this transition is not accompanied by any discontinuity. This especially holds for the centre of mass self-diffusion coefficient[4,31]. Rather, a three-section behaviour is proposed with respect to tube renewal (*Figure 2*). As mentioned previously, the three sections should lead to strong deviations of the transverse relaxation curves on approaching M_c. In fact, this tendency has been observed with polystyrene (PS 38 000 in Figure 1 of ref. 4). Unfortunately, the distributions of chain lengths also lead to non-exponential decays[22,32], so that this finding does verify but not prove the predicted behaviour (despite the small ratio $M_w/M_n=1.06$ of this sample). The same problem arises, in general, in trying to analyse the *shape* of the transverse relaxation curve in components due to different dynamic restrictions[32,33]. Additional experiments distinguishing the inner and outer chain sections, therefore, would be desirable in this context. Partial deuteration of the chains would be a suitable method for such a separation.

Several components of chain fluctuations have been defined. It is a crucial point that component A is of an *anisotropic* nature. Only the non-vanishing constant a_2 in equation (3) allows observation of further non-local processes. Anisotropic fluctuations are due to any type of restraints of the surrounding matrix. It is, therefore, this component which defines the diameter of the tube representing these restraints. The degree of anisotropy clearly indicates that the tube diameter must be near the mean nearest chain distance, so that component A involves any type of kink, crankshaft or torsional motion of a few segments which is compatible with this tube diameter. Only such a tight tube is suitable for the description of the n.m.r. results.

A tube of a diameter corresponding to the Doi–Edwards model[6] and the random coil assumption of the chain *inside* the tube contradicts the experimental fact, that non-local motions can be observed by n.m.r., i.e. by a method which directly 'sees' single segments rather than the whole chain or even the physical network. Note that the time scale of component A is many orders of magnitude below that of tube renewal. The latter nevertheless influences the n.m.r. relaxation times.

The separation of the diverse components can also be related to diverse scales of diffusive displacements. Component A virtually is not connected with translational segment displacements. Rather it concerns reorientations about the chain axis (*Figure 1*) caused, for example, by diffusing defects. The relevant defect displacements are of the order of a few segment lengths[4,5,9].

Translational displacements, however, are relevant for components B and C. Computer simulations showed[4,9] that the effective time and chain length dependences of the segment displacements depends on the scale considered. Hence, different curvilinear segment diffusion coefficients effective for the diverse processes are identified.

Component B refers to mean displacements of the order of the tight-tube orientation correlation length l. The effective diffusion coefficient, defined by:

$$D_1^{(l)}=\frac{l^2}{2\tau_l} \tag{19}$$

is then proportional to $M_w^{-0.5\pm0.3}$ according to equations (14) or (16). $D_1^{(l)}$ is insensitive to free-volume factors even at short chain-lengths[4].

Tube renewal by contour length fluctuation as the first part of component C is connected with larger displacements. The corresponding diffusion coefficient is defined (equation (9)) by:

$$D_1^{(0)}=\frac{4x_r^2}{\gamma_c\tau_r^c} \tag{20}$$

The relevant displacements are now of the order of x_r (equation (10)). For short chain-lengths, the molecular weight dependence of $D_1^{(0)}$ can be affected significantly by free volume[4].

Tube renewal by whole-chain reptation as the second part of component C is based on displacements of the order of the chain length. The curvilinear whole-chain diffusion coefficient (equation (7)) is:

$$D_1=\frac{(L_0-2x_r)^2}{\gamma_r\tau_r^r} \tag{21}$$

Model considerations[7,9] lead to the proportionality $D_1\sim M^{-1}$, which is compatible with equations (14) and (21).

Contour length fluctuation is considered to be based on growth and shrinkage of folds (*Figure 1*). It may be argued in context with diffusion of polymer stars[34] that fold formation is connected with a strong decrease in conformational entropy. In the present case, however, linear chains are considered, and fold formation at *any* position along the tube is effective for contour length fluctuation. Folds partially decouple the dynamics of the fragments between them. Additional degrees of translational freedom arise and, hence, the additional thermal energy connected with these translational degrees of freedom can compensate the reduction of conformational entropy.

An empirical indication of the partial decoupling by folds is given by melt transition data of straight-chain alkanes and their extrapolated values to infinite chain lengths[35]. The melting temperatures at 0.1 MPa obey:

$$\frac{1}{T_m}=\frac{1}{T_m^\infty}\left(1+\frac{6.86}{n}\right) \tag{22}$$

where $n(>10)$ is the (odd) number of carbon atoms per chain and $T_m^\infty=414.6$ K is the melting temperature in the limit of infinite chain lengths. The corresponding transition entropies obey:

$$\Delta S_m=\Delta s_\infty\left(2.5+n-\frac{30.2}{n}\right) \tag{23}$$

with $\Delta s_\infty=9.94$ J/K mol CH_2. The transition data also depend of course on the thermodynamic state of the crystals just below the melting temperature. For discussion purposes, however, it is sufficient to consider the crystalline state as a reference state *per se* for all chain lengths.

The fact that the transition data already approach their limits for infinite n for carbon numbers of the order of magnitude of 10 proves that then the units relevant for the melting transition are *shorter* than the total chain. The almost linear dependence of the transition entropy on the chain length also indicates approximately independent units. This is expected for chains consisting of dynamically decoupled fragments with an average length of the

order of magnitude of 10 methylene segments. Fold fluctuation might also explain the lateral displacements recently concluded from neutron scattering experiments[36].

ACKNOWLEDGEMENTS

This work has been supported by the Deutsche Forschungsgemeinschaft.

REFERENCES

1 Ferry, J. D. 'Viscoelastic Properties of Polymers', Wiley, New York, 1980
2 Bailey, R. T., North, A. M. and Pethrick, R. A. 'Molecular Motion in High Polymers', Clarendon Press, Oxford, 1981
3 Kimmich, R. and Hackenberg, L. 27th International Symposium on Macromolecules (IUPAC), Abstracts of Communications 1981, p. 858
4 Kimmich, R. and Bachus, R. *Colloid Polymer Sci.* 1982, **260**, 911
5 Voigt, G. and Kimmich, R. *Polymer* 1980, **21**, 1001
6 Doi, M. and Edwards, S. F. *J. Chem. Soc. Faraday Trans.* 1978, **II 74**, 1789
7 de Gennes, P. G. *J. Chem. Phys.* 1971, **55**, 572
8 Kimmich, R. *Colloid Polymer Sci.* 1974, **252**, 786; 1976, **254**, 918
9 Kimmich, R. and Doster, W. *J. Polymer Sci., Polymer Phys. Edn.* 1976, **14**, 1671
10 Kimmich, R. *Polymer* 1975, **16**, 851
11 Doi, M. *J. Polymer Sci., Polymer Letters Edn.* 1981, **19**, 265
12 Kimmich, R. *Polymer* 1977, **18**, 233
13 Rouse, P. E. *J. Chem. Phys.* 1953, **21**, 1272
14 Zimm, B. H. *J. Chem. Phys.* 1956, **24**, 269
15 Bueche, F. *J. Chem. Phys.* 1954, **22**, 603
16 Kimmich, R. *Z. Naturforsch.* 1976, **31a**, 693
17 Abragam, A. 'The Principles of Nuclear Magnetism', Clarendon Press, Oxford, 1961
18 Graessley, W. W. *Adv. Polymer Sci.* 1982, **47**, 67
19 Kimmich, R. *Polymer Preprints* 1981, **22/1**, 109
20 Lastovka, J. B. and Benedek, G. B. *Phys. Rev. Letters* 1966, **17**, 1039
21 Mountain, R. D. *Rev. Modern Phys.* 1966, **38**, 205
22 Koch, H., Bachus, R. and Kimmich, R. *Polymer* 1980, **21**, 1009
23 Doolittle, A. K. *J. Appl. Physics* 1951, **22**, 1471
24 Fox, T. G., Gratch, S. and Lashaek, S. 'Rheology' (Ed. F. R. Eirich), Academic Press, New York, 1956, Vol. 1, p. 431
25 Doi, M. *Chem. Phys. Letters* 1974, **26**, 269
26 Allen, V. R. and Fox, T. G. *J. Chem. Phys.* 1964, **41**, 337
27 Doolittle, A. G. *J. Appl. Phys.* 1951, **22**, 1031
28 Peticolas, W. L. and Watkins, J. M. *J. Am. Chem. Soc.* 1957, **79**, 5083
29 Tung, L. H. *J. Polymer Sci.* 1960, **46**, 409
30 Porter, R. S. and Johnson, J. F. *J. Appl. Polymer Sci.* 1960, **3**, 194
31 Bachus, R. and Kimmich, R. *Polymer* 1983, **24**, 964
32 Folland, R. and Charlesby, A. *J. Polymer Sci., Polymer Letters Edn.* 1978, **16**, 339
33 Cohen-Addad, J. P. *J. Physique* 1982, **43**, 1509
34 de Gennes, P. G. *J. Physique* 1975, **36**, 1199
35 Dollhopf, W., Grossmann, H. P. and Leute, U. *Colloid Polymer Sci.* 1981, **259**, 267
36 Richter, D., Baumgärtner, A., Binder, K., Ewen, B. and Hayter, J. B. *Phys. Rev. Letters* 1981, **47**, 109